



## ORIGINAL ARTICLE

# Multiplexed flow cytometric approach for detection of anti-SARS-CoV-2 IgG, IgM and IgA using beads covalently coupled to the nucleocapsid protein

I.F. Zattoni<sup>1</sup>, L.F. Huergo<sup>2</sup>, E.C.M. Gerhardt<sup>3</sup>, J.M. Nardin<sup>4</sup>, A.M.F. dos Santos<sup>4</sup>, F.G.M. Rego<sup>5</sup>, G. Picheth<sup>5</sup>, V.R. Moure<sup>1,5</sup>  and G. Valdameri<sup>1,5</sup> 

1 Pharmaceutical Sciences Graduate Program, Laboratory of Cancer Drug Resistance, Federal University of Paraná, Curitiba, PR, Brazil

2 Setor Litoral, Federal University of Paraná, Matinhos, PR, Brazil

3 Department of Biochemistry and Molecular Biology, Federal University of Paraná, Curitiba, PR, Brazil

4 Hospital Erasto Gaertner, Curitiba, PR, Brazil

5 Department of Clinical Analysis, Federal University of Paraná, Curitiba, PR, Brazil

**Significance and Impact of the Study:** Flow cytometry has emerged as a promising technique for detection of anti-SARS-CoV-2 antibodies. In this study, we developed an innovative strategy for simultaneous detection of immunoglobulin G (IgG), IgM and IgA. This new cell-free assay efficiently discriminates COVID-19 negative and positive samples. The simultaneous detection of IgG, IgM and IgA showed a high sensitivity and specificity. This novel strategy opens a new avenue for flow cytometry-based diagnosis.

## Keywords

CBA functional beads, COVID-19, flow cytometry, IgG, IgM and IgA antibodies, multiplex immunoassay, SARS-CoV-2.

## Correspondence

Vivian Rotuno Moure and Glaucio Valdameri, Pharmaceutical Sciences Graduate Program, Laboratory of Cancer Drug Resistance, Federal University of Paraná, 80210-170 Curitiba, PR, Brazil.

E-mail: vivian.moure@ufpr.br and gvaldameri@ufpr.br

2021/0040: received 28 June 2021, revised 11 January 2022 and accepted 13 January 2022

doi:10.1111/lam.13674

## Abstract

Flow cytometry has emerged as a promising technique for detection of SARS-CoV-2 antibodies. In this study, we developed an innovative strategy for simultaneous detection of immunoglobulin G (IgG), IgM and IgA. The SARS-CoV-2 nucleocapsid protein was covalently bound to functional beads surface applying sulpho-SMCC chemistry. BUV395 anti-IgG, BB515 anti-IgM, biotinylated anti-IgA1/IgA2 and BV421 streptavidin were used as fluorophore conjugated secondary antibodies. Serum and antibodies reaction conditions were optimized for each antibody isotype detection and a multiplexed detection assay was developed. This new cell-free assay efficiently discriminates COVID-19 negative and positive samples. The simultaneous detection of IgG, IgM and IgA showed a sensitivity of 88.5–96.2% and specificity of 100%. This novel strategy opens a new avenue for flow cytometry-based diagnosis.

## Introduction

The first case of the novel coronavirus, SARS-CoV-2, which causes a disease known as COVID-19, was reported in Wuhan, China, on 31 December 2019. The World Health Organization (WHO), on 11 March 2020, declared COVID-19 a pandemic. The course of the COVID-19 pandemic is a consequence of the rapid spread of this virus and, more recently, the emergency of novel variants (Hu *et al.* 2020).

The understanding of immune response to SARS-CoV-2 infection is critical, especially in discrimination of disease severity and vaccine efficacy. Although the antibody response to COVID-19 are not fully characterized, it is well-known that seroconversion for IgG and IgM occurs typically within 3 weeks, being simultaneously or sequentially, initiating 5 days after symptom onset (Yu *et al.* 2020), with a median day of seroconversion of 13 days post symptom onset for both IgG and IgM (Long *et al.* 2020).

The IgA isotype have gained attention in COVID-19 (Russell *et al.* 2020). The secretory form would primarily act at the virus entry site (Chao *et al.* 2020) and the circulating anti-receptor-binding domain (RBD) IgA has been revealed as neutralizing antibody (Sterlin *et al.* 2021; Zeng *et al.* 2021). In addition, circulating IgA levels has also been correlated with disease severity (Grossberg *et al.* 2021). IgA seroconversion appears as early as IgG and IgM (Norman *et al.* 2020), or slightly early than IgG and IgM (Padoan *et al.* 2020; Yu *et al.* 2020).

These multiple antibody isotypes target viral proteins, including spike subunit 1 (S1) and subunit 2 (S2), receptor-binding domain (RBD), Cys-like protease (Mpro) and nucleocapsid (or nucleoprotein) (Meyer *et al.* 2014; Chang *et al.* 2020; Cáceres-Martell *et al.* 2021). Several studies described the detection of SARS-CoV-2-specific IgG and IgM (Hachim *et al.* 2020; Long *et al.* 2020; Okba *et al.* 2020; Petherick, 2020; Vashist, 2020; Yu *et al.* 2020; de Assis *et al.* 2021; Egia-Mendikute *et al.* 2021; Huergo *et al.* 2021; Mariën *et al.* 2021), while the detection of SARS-CoV-2-specific IgA has been less reported (Behrens *et al.* 2020; Norman *et al.* 2020; Okba *et al.* 2020; Padoan *et al.* 2020; Munitz *et al.* 2021; Sterlin *et al.* 2021). In most cases, antibody detection is based on ELISA or chemiluminescent assays.

Recent studies have exploited flow cytometry to develop assays to detect COVID-19 seroconversion in humans. In five studies, the spike protein was overexpressed on the surface of cells, allowing the detection of antibodies in patient samples using fluorescent secondary anti-antibodies (Lapuente *et al.* 2020; Anand *et al.* 2021; Goh *et al.* 2021; Horndler *et al.* 2021; Simard *et al.* 2022). In other studies, SARS-CoV-2 antigens were either non-covalently bound to beads coated with streptavidin (Dogan *et al.* 2021; Egia-Mendikute *et al.* 2021) or covalently coupled to magnetic fluorescent beads (Cáceres-Martell *et al.* 2021).

Most of immunological assays detect the antibodies against spike protein, showing a limited use in differentiating infected individuals that those immunized by vaccination, since the main COVID-19 vaccines used worldwide are spike-targeted (Dörschug *et al.* 2021; Forni and Mantovani 2021). Considering the immunogenic response against the nucleocapsid protein (Leung *et al.* 2004; Zhu *et al.* 2006; Grzelak *et al.* 2020; To *et al.* 2020) and the similar profile of IgG and IgA against nucleocapsid and spike proteins (Sterlin *et al.* 2021), the goal of this work was to develop an assay for the detection of antibodies initially to target the SARS-CoV-2 nucleocapsid protein. To pursue this, SARS-CoV-2 nucleocapsid antigen was covalently linked to functional beads (CBA), which allowed accurate multiplexed detection of IgG, IgM and IgA isotypes using flow cytometry.

## Results and discussion

### Strategy at a glance

Cytometric bead array (CBA) is called functional beads by the producer and compatible with flow cytometry. These fluorescent beads have been widely used to investigate antigens in serum samples. There are several commercially available beads which are covalently covered by antibodies that recognize specific targets. Detection of the analyte using flow cytometry is performed using a fluorochrome-conjugated secondary antibodies. Despite this well-established approach, the application of these CBA beads to covalently bind antigens and investigation of antibodies is poorly studied (Morgan *et al.* 2004). In this work, thiol groups of the commercial fluorescent polystyrene naked CBA beads were reduced to the active sulphhydryl form by DTT. The recombinant 6xHis-tagged SARS-CoV-2 nucleocapsid protein solubilized on PBS was covalently bound to CBA beads by sulpho-SMCC chemistry (Fig. 1a). These functionalized beads were named as CBA-N. CBA-N was further used as proof of concept to investigate the presence of IgG, IgM and IgA isotypes in COVID-19 positive serum samples. To allow antibodies detection, specific anti-human IgG and IgM conjugated with BD Horizon BUV395 and BD Horizon BB515 fluorochromes, respectively, were used. Biotinylated anti-human IgA1/IgA2 and streptavidin conjugated with BD Horizon BV421 was used as a second-step reagent to improve the sensitivity of IgA detection (Fig. 1b).

The prepared CBA-N was homogeneously distributed with a diameter size of 7.5 µm, which allowed recognition by flow cytometry according to the forward (FSC) and side scatter (SSC) parameters and using a specific gate (Fig. 1c). All fluorochromes were rationally chosen to attenuate the spillover of fluorescence in a multiplex system, since each fluorochrome is excited by a different laser. This combination of fluorochromes was optimized for a flow cytometer equipped with at least three lasers, including a 355, 405 and 488 nm lasers. As shown in Fig. 1c, the fluorescence was recorded simultaneously using three different channels.

To achieve the best standardization for multiplexed detection of IgG, IgM and IgA response to SARS-CoV-2 infection, the conditions for each antibody response were optimized.

### Optimization of conditions

Negative samples were obtained before the pandemic and were called as control (Ctrl). COVID-19 positive samples were obtained of patients from an oncological hospital (HEG) at Curitiba after 14 days of hospitalization, which correspond to approximately 19 days after the symptom

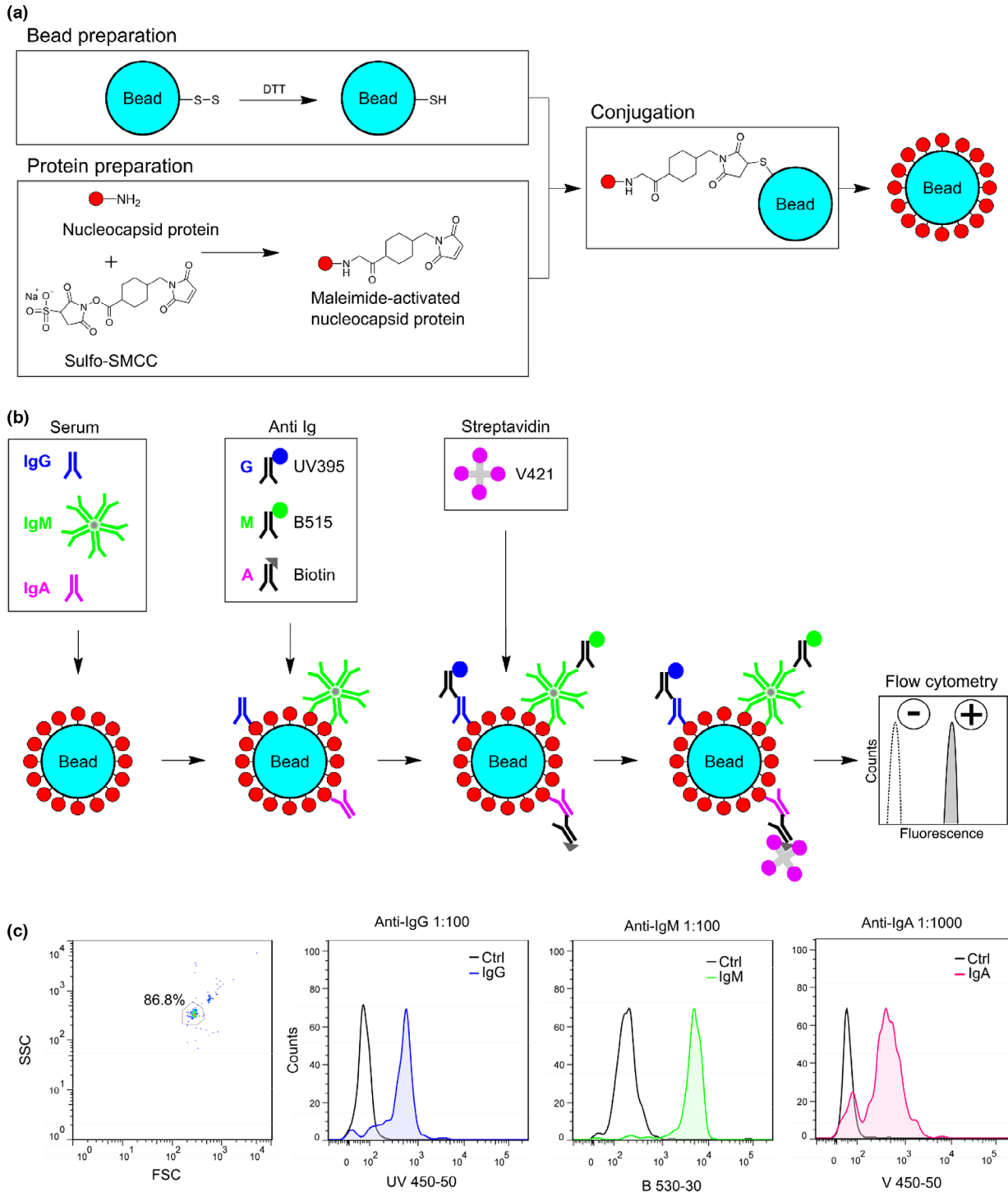


**Figure 1** Rational strategy overview. (a) Fluorescent polystyrene beads of 7.5 µm reduced by DTT. SARS-CoV-2 nucleocapsid protein solubilized in PBS covalently bound to beads surface by sulpho-SMCC chemistry to originate functionalized beads named as CBA-N. (b) Schematic representation of the multiplex assay. (c) Gate selection based on bead size. Representative histograms of COVID-19 positive samples

onset. These patients were diagnosed with COVID-19 by RT-PCR showing positive results from two independent laboratories (data not shown), and most samples are from

oncologic patients. For standardization of the assay, we used a mixture of, at least three, negative and positive samples.

The data were expressed as the percentage of positive fluorescent beads (PPFB). As shown in Fig. 2a, a serum dilution curve revealed that the discrimination of positive vs negative IgG samples was achieved at a serum dilution of 1000-fold. A possible hook effect was observed in undiluted until 1 : 100 diluted serum specimens. However, additional studies are required to understand this phenomenon. After setting the appropriate serum dilution (1000-fold), a range of fluorochrome conjugate (anti-IgG UV395) dilutions was evaluated. The data showed that the best results were obtained using the anti-IgG diluted 100-fold (Fig. 2b). The same rational strategy was carried out for IgM and IgA detection. The IgM detection was only able to discriminate between COVID-19 positive and negative samples when a serum dilution of 1000-fold was applied (Fig. 2c). For IgM detection, the optimized combination was with serum diluted 1000-fold and the anti-IgM B515 diluted 100-fold (Fig. 2c,d). IgA detection showed a different pattern, probably because the biotin-streptavidin system used. As shown in Fig. 2e, the best serum dilutions were between 10 and 100-fold. However, the serum 1000-fold diluted was also able to discriminate between negative and positive samples. Envisioning a multiplexed antibody detection, we decided to use 1000-fold serum dilution for the evaluation of anti-IgA curve. The anti-IgA showed similar results with secondary antibody used at dilution between 100 and 1000-fold (Fig. 2f). In addition, the anti-IgA dilution result was confirmed using the serum 10-fold diluted (data not shown).

An estimation of analytical coefficient of variation (CVa) for imprecision (inter-assay;  $n = 12$ ) was calculated using PPFB (%) values from serum pools of controls (mean  $2.0 \pm 2.0$ ) and COVID-19 positive (IgG, IgM and IgA combined; mean  $69.7 \pm 19.2$ ) samples, showing a CVa values of 100 and 27.5%, respectively.

### Proof of concept

After characterization of the optimized conditions for single antibody isotype detection, double and triple staining were performed. The results demonstrated the absence of fluorescence spillover (data not shown), confirming the feasibility of the experimental design for multiplex detection. The combination of lasers UV355 nm, V405 nm and blue 488 nm with UV395, V421 and B515 fluorochromes allowed discriminating negative vs positive samples for the simultaneous detection of IgG, IgA and IgM, respectively, without any compensation. Three independent beads preparations were tested, showing similar results (data not shown).

Finally, the multiplexed approach was used to evaluate a panel of negative ( $n = 10$ ) and COVID-19 positive

( $n = 26$ ) samples (Fig. 3 and Fig. S1). Receiver operating characteristic (ROC)-established cutoff was used for discrimination of negative and COVID-19 positive samples. The specificity of 100% was achieved for all isotypes. The sensitivity was 88.5% for the detection of IgG, 92.3% for IgM and 96.2% for IgA. The area under the ROC curve was calculated as 0.946, 0.950 and 0.962 for IgG, IgM and IgA, respectively (Fig. 3 and Table S1). Venn diagram analysis showed that 22/26 presented IgG, IgM and IgA, 1/26 presented only IgG and IgA, and 2/26 presented only IgM and IgA. None of the positive samples presented only IgG and IgM, and 1/26 did not present any of the antibodies studied (Fig. 3d).

Flow cytometry is described as an important analytical tool for immunological assays. Commercially available CBA functional beads are widely used for the evaluation of multiple analytes in a single sample. For instance, several papers have described the use of CBA bound to specific antibodies for the detection and quantification of a large variety of human cytokines (Morgan *et al.* 2004) using a non-competing secondary antibody for detection.

The application of flow cytometry in COVID-19 has exploited the use of cell-based assays for detection of IgM, IgA, and IgG subclasses against the SARS-CoV-2 S protein. However, most of these studies targeted a single antibody detection (Lapuente *et al.* 2020; Anand *et al.* 2021; Goh *et al.* 2021; Horndler *et al.* 2021; Simard *et al.* 2022). To the best of our knowledge, there is only three studies employing a cell-free flow cytometric approach to evaluate the humoral immune response (Cáceres-Martell *et al.* 2021; Dogan *et al.* 2021; Egia-Mendikute *et al.* 2021). In two cases, the authors used fluorescent beads coated with streptavidin, which allow the binding on biotinylated SARS-CoV-2 antigens to detect antibodies. Egia-Mendikute *et al.* (2021) showed a simultaneous detection of IgG and IgM against SARS-CoV-2 antigens. Unexpectedly, the authors detected nucleocapsid IgG in controls pre-pandemic samples (Egia-Mendikute *et al.* 2021), which is in sharp contrast to the literature (Grossberg *et al.* 2021; Huergo *et al.* 2021; Mariën *et al.* 2021; Munitz *et al.* 2021). As reported by Dogan *et al.* (2021), the binding of each antigen to a different fluorescent bead allowed the singleplex detection of multiple antibody isotypes, as IgG1-4, IgM and IgA. However, the use of all secondary antibodies conjugated to phycoerythrin unmet the inherent advantage of flow cytometry for simultaneous serum antibody detection. Furthermore, it has been recognized that the detection of one antibody isotype alone has a limited value for COVID-19 diagnosis and monitoring (Escribano *et al.* 2020). More recently, four SARS-CoV-2 antigens (spike, RBD, nucleocapsid and MPro) were covalently coupled to magnetic fluorescent beads containing a high-density carboxyl functional group

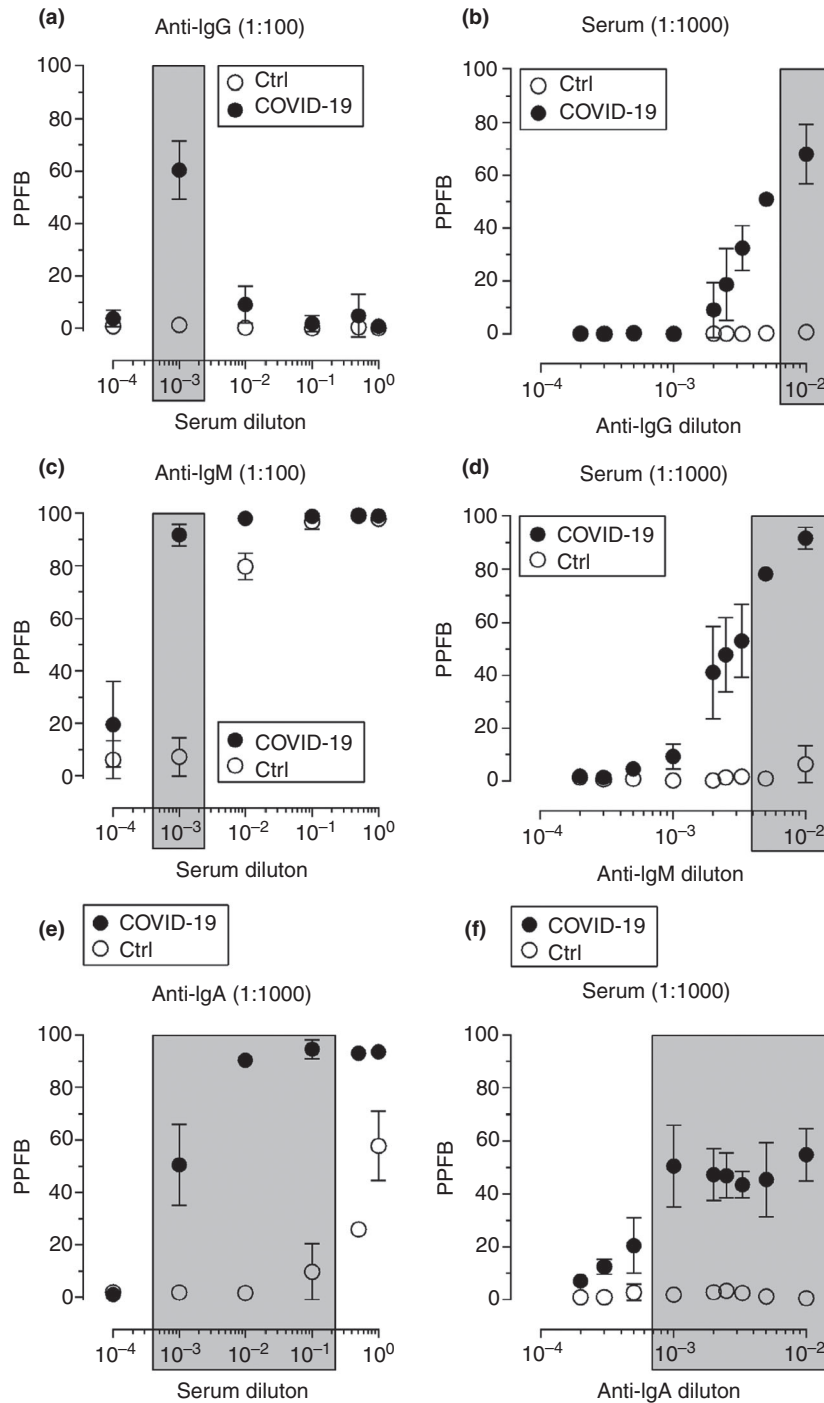


**Figure 2** Serum and antibody dilution. Determination of percentage of positive fluorescent beads (PPFB) by flow cytometry using CBA-N beads. (a) Serum dilution using anti-IgG diluted 100-fold. (b) Anti-IgG dilution using serum diluted 1000-fold. (c) Serum dilution using anti-IgM diluted 100-fold. (d) Anti-IgM dilution using serum diluted 1000-fold. (e) Serum dilution using anti-IgA diluted 1000-fold. (f) Anti-IgA dilution using serum diluted 1000-fold. A mix of three samples were used. Data are representative of at least two independent experiments and values are expressed in mean  $\pm$  SD.

on the surface. These beads were used for simultaneous detection of IgG, IgM and IgA by flow cytometry, showing results with low background signals and high

specificity and sensitivity (Cáceres-Martell *et al.* 2021). However, magnetic beads are not compatible with certain flow cytometers.

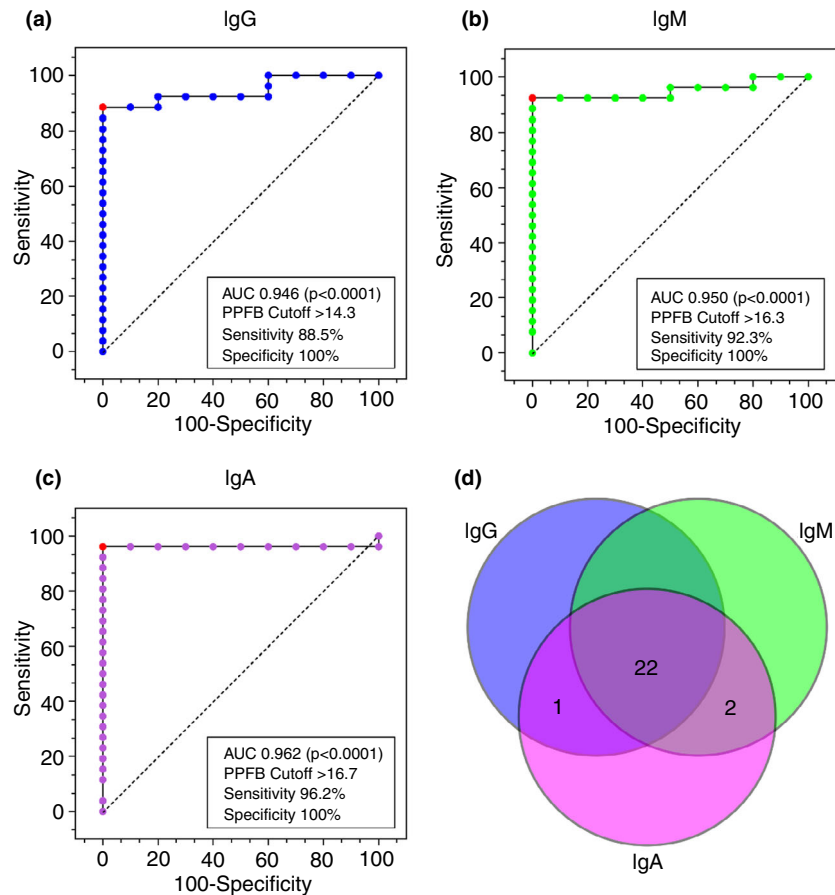


**Figure 3** Receiver operating characteristic (ROC) curves and Venn diagram. COVID-19 negative controls ( $n = 10$ ) and positive ( $n = 26$ ). ROC curve for (a) IgG. (b) IgM. (c) IgA. AUC, area under de curve; PPFB, percentage of positive fluorescent beads (%); red point, highest Youden index (cutoff). (d) Venn diagram of COVID-19 positive samples simultaneously compared with the detection of IgG, IgM and IgA. The statistical calculations were performed using MedCalc v.7.12.7.2.0 (MedCal Software bvba)

In our study, the binding of SARS-CoV-2 nucleocapsid protein to CBA functional beads was covalent (Fig. 1), which offers advantages of more robust surface, higher density of epitopes and orientation to maximize epitopes exposing and complementary binding (Welch *et al.* 2017). We provided a proof of concept of a cell-free multiplex assay based on flow cytometry for immunological diagnosis of COVID-19 (Fig. 1). The novel method allowed accurate discrimination between COVID-19 positive samples and pre-pandemic negative controls using standardized conditions (Figs 2 and 3). Specificity of 100% and sensitivity of 88.5, 92.3 and 96.2% for IgG, IgM and IgA, respectively, were determined (Fig. 3 and Table S1). The IgG results were confirmed by a magnetic bead-based immunoassay (Fig. S1b) (Huergo *et al.* 2021). The results of our method for IgG and IgM showed both sensitivity and specificity similar to the FDA-approved tests (sensitivity 61–98% and specificity 90–100%) (Sen-Crowe *et al.* 2021). The detection of IgA showed increased sensitivity

and specificity in comparison to a commercial test based on ELISA (Euroimmun<sup>TM</sup>, 82.9% and 82.2%) (Cota *et al.* 2020). Interestingly, the combined IgG, IgM and IgA analysis improved the serological diagnosis. Most of the RT-PCR positive samples presented the three antibody isotypes and, at least, two antibody isotypes were detected from 25/26 (Fig. 3d and Fig. S1). The single negative result was from patient 394 (Fig. S1), who was presenting severe myelosuppression after chemotherapy in the day of the blood sample collection. It should be considered that the small number of samples may affect the statistical analysis. Hence, a large cohort will be necessary to confirm the results.

Several studies have demonstrated the superiority of multiplex approaches for COVID-19 immunological response addressing both multiple antigens and multiple isotypes of antibodies. Among them, the Luminex Platform is the most used: for the detection of IgG using microspheres coupled with S1, RBD and nucleocapsid

protein (den Hartog *et al.* 2020), the detection of IgG, IgM and IgA against several antigens including non-structural proteins, spike and nucleocapsid (Butt *et al.* 2021) and total antibodies (IgG/IgM/IgA) against the S1, RBD and nucleocapsid antigens (Fotis *et al.* 2021). Other multiplex approaches target the detection of IgG antibody against SARS-CoV-2 antigens were also described, such as a flow-based chemiluminescence microarray immunoassay (CL-MIA) (Klöpffel *et al.* 2021) and the VaxArray Coronavirus SeroAssay Kit (Dawson *et al.* 2021).

A special strength of the present study is the availability of a large repertoire of combinations of multiple antigens covalent bound to each set of fluorescent CBA beads, which allows detection of unique optical signatures using conventional flow cytometers. Therefore, the multiplexed flow cytometric-based tool presented here provided a blueprint for rapid development of antibody evaluation to others emerging infections. In summary, our data present a flow cytometric bead-based assay that offers a cost-effective alternative to multiplex determination of IgG, IgM and IgA response in COVID-19, as a proof concept for further studies.

## Materials and methods

### Chemicals and antibodies

The cytometric bead array (CBA) polystyrene beads (cat n° 560037), coupling buffer BD<sup>TM</sup> (cat n° 51-9004756), storage buffer BD<sup>TM</sup> (cat n° 51-9004758) and wash buffer BD<sup>TM</sup> (cat n° 51-9003798) were purchased from BD Biosciences (Franklin Lakes, NJ, USA). Bovine serum albumin (BSA, A8022), 4-(N-maleimidomethyl)cyclohexane-1-carboxylic acid 3-sulpho-N-hydroxysuccinimide ester sodium salt – sulpho-SMCC (M6035), N-ethylmaleimide (E3876) and dithiothreitol (DTT, 1019777001) were purchased from Sigma-Aldrich. Phosphate buffer saline (PBS) 10x pH 7.2 (70013-032) was purchased from Gibco. Antibodies brilliant ultraviolet (BUV395) mouse anti-human IgG (cat n° 564229), brilliant blue (BB515) mouse anti-human IgM (cat n° 564622), biotin mouse anti-human IgA1/IgA2 (cat n° 555884), and brilliant violet (BV421) streptavidin (cat n° 563259) were purchased from BD Biosciences.

### Antigen preparation and beads conjugation

Expression and purification of recombinant SARS-CoV-2 nucleocapsid protein was performed as described previously (Huergo *et al.* 2021). The coupling reaction was performed as described by the manufacturer with modifications. Initially, beads and antigen were prepared. CBA E5 beads were resuspended by vortex for 30 s. Then 75 µl

of E5 beads were collected and sonicated for 60 s. After that, 1.9 µl of DTT 1 mol l<sup>-1</sup> was added, mixed with vortex and placed on horizontal shaker for 1 h at room temperature. Then, 1 ml of coupling buffer BD<sup>TM</sup> was added, mixed, centrifuged at 2000 g for 3 min and the supernatant discarded. This washing step was repeated three times. Finally, the CBA beads were resuspended in coupling buffer to next step. In parallel, 90 µg of protein in PBS (1×) was mixed with 2 µl of sulpho-SMCC 2 mg ml<sup>-1</sup>. The mixture was placed on horizontal shaker for 1 h at room temperature (25°C).

The maleimide-activated nucleocapsid protein was transferred to the tube containing the prepared beads. The components were mixed in vortex and incubated under agitation for 1 h at room temperature. After this period, 2 µl of N-ethylmaleimide 2 mg ml<sup>-1</sup> were added and kept under agitation for 15 min at room temperature. Then, 1 ml of storage buffer BD<sup>TM</sup> was added, mixed, centrifuged at 2000 g for 3 min and the supernatant was discarded. This washing step was repeated three times. After this, the conjugated beads were resuspended in 500 µl of storage buffer and kept at 4°C. The functionalized beads were stable for, at least, 2 months.

### Samples

Human serum and EDTA-plasma were collected at Hospital Erasto Gaertner (HEG), a cancer reference centre where both oncological and non-oncological COVID-19 positive patients have been admitted. This study was approved by the Ethics Committee of HEG (CEP/HEG: 31592620.4.1001.0098). The samples consisted of 10 pre-pandemic, considered as COVID-19 negative or control, and 26 COVID-19 positive, being 18 from oncologic patients and 8 from non-oncologic patients. From 18 patients with cancer, 13 were patients with solid tumors and 5 were patients with haematological malignancies. Only 5 from 18 patients received any treatment 90 days before diagnosis of COVID-19. One received chemotherapy (patient 394), two radiotherapy and two a surgical procedure. Only 2 from 18 patients were in palliative care. Three of the oncologic patients were leukopenic (<4000 cells per mm<sup>3</sup>) and 15 were lymphopenic (values <25% or <1000 cells per mm<sup>3</sup>). The mean lymphocytes % count for those patients were 13.3%. For non-oncologic patients, only one was leukopenic (920 cells per mm<sup>3</sup>) and 6 were lymphopenic (mean lymphocytes % was 17.8). From the total of 26 patients diagnosed with COVID-19, only 4 were neutropenic (<500 cells per mm<sup>3</sup>), 2 oncologic and 2 non-oncologic patients. COVID-19 positive samples were diagnosed by the detection of SARS-CoV-2 RNA using RT-PCR from nasopharyngeal sample swabs by two independent laboratories.

COVID-19 positive samples were collected 14 days after hospitalization, with varied time of the appearance of first symptoms (14–31 days).

### Staining and analysis

A suspension of conjugated beads was prepared following the proportion of 1 µl of stock suspension conjugated beads to 50 µl of wash buffer BD<sup>TM</sup>. Then, 50 µl of diluted beads were mixed with serum or EDTA-plasma (pure or diluted with PBS 1× containing BSA 0.5%) and incubated at room temperature for 90 min. Then, beads were centrifuged at 4000 g for 5 min. The supernatant was removed and 300 µl of PBS/BSA 0.5% was added and mixed with vortex followed by centrifugation at 4000 g for 5 min (this step was performed twice). After that, 50 µl of diluted antibody was added and incubated for 90 min (the antibody range used was 1 : 100, 1 : 200, 1 : 300, 1 : 400, 1 : 500, 1 : 1000, 1 : 2000, 1 : 3000 and 1 : 5000). After this time, beads were centrifuged at 4000 g for 5 min and washed twice with 300 µl of PBS/BSA 0.5%. For IgG and IgM detection, the samples were resuspended in PBS and analysed by flow cytometry using UV450/50 filter for IgG and B530/30 filter for IgM. For IgA analysis, a further incubation was performed with 50 µl of streptavidin 1 : 100 for 90 min at room temperature (25°C). The samples were centrifuged and washed twice with PBS/BSA 0.5%, resuspended in PBS and analysed by flow cytometry using V450/50 filter.

For multiplex analysis, diluted beads were incubated with serum 1 : 1000 for 90 min and washed as previously described. Then a single solution was made with IgG (1 : 100), IgM (1 : 100) and IgA (1 : 1000). A volume of 50 µl of antibody mixture was incubated with beads for 90 min and washed. After that, the incubation with streptavidin (1 : 100) was performed for 90 min and washed. The beads were resuspended in PBS and analysed using a BD FACS Celesta<sup>TM</sup> equipped with three lasers (355, 405 and 488 nm) using UV450/50, V450/50 and B530/30 filters. The data were expressed as the percentage of positive fluorescent beads (PPFB), as previously described (Gama Ker *et al.* 2013). Statistical analysis based on receiver operating characteristic (ROC) curve was used to determine cutoff, sensitivity, specificity and area under curve (AUC) using MedCalc v.7.12.7.2.0 (MedCal Software bvba).

### Acknowledgements

The authors thank Andréa Teixeira-Carvalho for the discussion about CBA covalent immobilization. This work was supported by CNPq (grant number 400953/2016-1) and Coordenação de Aperfeiçoamento de Pessoal de Nível Superior – Brasil (CAPES) (Finance code 001).

### Conflict of Interest

No conflict of interest declared.

### Author contributions

V.R.M and G.V conceived and designed the study. L.F.H and E.C.M.G contributed with the nucleocapsid protein. J.M.N and A.M.F.S contributed with samples. F.G.M.R and G.P performed the statistical analysis. I.F.Z and G.V performed the experiments. I.F.Z, G.P, V.R.M and G.V analyzed the data. V.R.M and G.V wrote the paper with the help of I.F.Z, L.F.H and G.P.

### References

- Anand, S.P., Prévost, J., Richard, J., Perreault, J., Tremblay, T., Drouin, M., Fournier, M.-J., Lewin, A. *et al.* (2021) High-throughput detection of antibodies targeting the SARS-CoV-2 Spike in longitudinal convalescent plasma samples. *Transfusion* **61**, 1377–1382.
- de Assis, R.R., Jain, A., Nakajima, R., Jasinskas, A., Felgner, J., Obiero, J.M., Norris, P.J., Stone, M. *et al.* (2021) Analysis of SARS-CoV-2 antibodies in COVID-19 convalescent blood using a coronavirus antigen microarray. *Nat Commun* **12**, 1–9.
- Behrens, G.M.N., Cossmann, A., Stankov, M.V., Witte, T., Ernst, D., Happle, C. and Jablonka, A. (2020) Perceived versus proven SARS-CoV-2-specific immune responses in health-care professionals. *Infection* **48**, 631–634.
- Butt, J., Murugan, R., Hippchen, T., Olberg, S., van Straaten, M., Wardemann, H., Stebbins, E., Kräusslich, H.-G. *et al.* (2021) From multiplex serology to serolomics—a novel approach to the antibody response against the SARS-CoV-2 proteome. *Viruses* **13**, 749–766.
- Cáceres-Martell, Y., Fernández-Soto, D., Campos-Silva, C., García-Cuesta, E.M., Casasnovas, J.M., Navas-Herrera, D., Beneítez-Martínez, A., Martínez-Fleta, P. *et al.* (2021) Single-reaction multi-antigen serological test for comprehensive evaluation of SARS-CoV-2 patients by flow cytometry. *Eur J Immunol* **51**, 2633–2640.
- Chang, F.-Y., Chen, H.-C., Chen, P.-J., Ho, M.-S., Hsieh, S.-L., Lin, J.-C., Liu, F.-T. and Sytwu, H.-K. (2020) Immunologic aspects of characteristics, diagnosis, and treatment of coronavirus disease 2019 (COVID-19). *J Biomed Sci* **27**, 1–13.
- Chao, Y.X., Röttschke, O. and Tan, E.K. (2020) The role of IgA in COVID-19. *Brain Behav Immun* **87**, 182–183.
- Cota, G., Freire, M.L., de Souza, C.S., Pedras, M.J., Saliba, J.W., Faria, V., Alves, L.L., Rabello, A. *et al.* (2020) Diagnostic performance of commercially available COVID-19 serology tests in Brazil. *Int J Infect Dis* **101**, 382–390.
- Dawson, E.D., Kuck, L.R., Blair, R.H., Taylor, A.W., Toth, E., Knight, V. and Rowlen, K.L. (2021) Multiplexed,



- microscale, microarray-based serological assay for antibodies against all human-relevant coronaviruses. *J Virol Methods* **291**, 1–10.
- Dogan, M., Kozhaya, L., Placek, L., Gunter, C., Yigit, M., Hardy, R., Plassmeyer, M., Coatney, P. et al. (2021) SARS-CoV-2 specific antibody and neutralization assays reveal the wide range of the humoral immune response to virus. *Commun Biol* **4**, 1–13.
- Dörschug, A., Frickmann, H., Schwanbeck, J., Yilmaz, E., Mese, K., Hahn, A., Groß, U. and Zautner, A.E. (2021) Comparative assessment of sera from individuals after S-gene RNA-based SARS-CoV-2 vaccination with spike-protein-based and nucleocapsid-based serological assays. *Diagnostics* **11**, 426–443.
- Egia-Mendikute, L., Bosch, A., Prieto-Fernández, E., Lee, S.Y., Jiménez-Lasheras, B., García del Río, A., Antoñana-Vildosola, A., Bruzzone, C. et al. (2021) Sensitive detection of SARS-CoV-2 seroconversion by flow cytometry reveals the presence of nucleoprotein-reactive antibodies in unexposed individuals. *Commun Biol* **4**, 1–10.
- Escribano, P., Álvarez-Uría, A., Alonso, R., Catalán, P., Alcalá, L., Muñoz, P. and Guinea, J. (2020) Detection of SARS-CoV-2 antibodies is insufficient for the diagnosis of active or cured COVID-19. *Sci Rep* **10**, 1–7.
- Forni, G. and Mantovani, A. (2021) COVID-19 vaccines: where we stand and challenges ahead. *Cell Death Differ* **28**, 626–639.
- Fotis, C., Meimetis, N., Tsolakos, N., Politou, M., Akinosoglou, K., Pliaka, V., Minia, A., Terpos, E. (2021) Accurate SARS-CoV-2 seroprevalence surveys require robust multi-antigen assays. *Sci Rep* **11**, 1–11.
- Gama Ker, H., Dian de Oliveira Aguiar-Soares, R., Mendes Roatt, B., das Dores Moreira, N., Coura-Vital, W., Martins Carneiro, C., Teixeira-Carvalho, A., Assis Martins-Filho, O. et al. (2013) Effect of the preservative and temperature conditions on the stability of *Leishmania infantum* promastigotes antigens applied in a flow cytometry diagnostic method for canine visceral leishmaniasis. *Diagn Microbiol Infect Dis* **76**, 470–476.
- Goh, Y.S., Chavatte, J.-M., Lim Jieling, A., Lee, B., Hor, P.X., Amrun, S.N., Lee, C.-P., Chee, R.-L. et al. (2021) Sensitive detection of total anti-Spike antibodies and isotype switching in asymptomatic and symptomatic individuals with COVID-19. *Cell Rep Med* **2**, 1–10.
- Grossberg, A.N., Koza, L.A., Ledreux, A., Prusmack, C., Krishnamurthy, H.K., Jayaraman, V., Granholm, A.-C. and Linseman, D.A. (2021) A multiplex chemiluminescent immunoassay for serological profiling of COVID-19-positive symptomatic and asymptomatic patients. *Nat Commun* **12**, 1–11.
- Grzelak, L., Temmam, S., Planchais, C., Demeret, C., Tondeur, L., Huon, C., Guivel-Benhassine, F., Staropoli, I. et al. (2020) A comparison of four serological assays for detecting anti-SARS-CoV-2 antibodies in human serum samples from different populations. *Sci Transl Med* **12**, 1–13.
- Hachim, A., Kavian, N., Cohen, C.A., Chin, A.W.H., Chu, D.K.W., Mok, C.K.P., Tsang, O.T.Y., Yeung, Y.C. et al. (2020) ORF8 and ORF3b antibodies are accurate serological markers of early and late SARS-CoV-2 infection. *Nat Immunol* **21**, 1293–1301.
- den Hartog, G., Schepp, R.M., Kuijper, M., GeurtsvanKessel, C., van Beek, J., Rots, N., Koopmans, M.P.G., van der Klis, F.R.M. et al. (2020) SARS-CoV-2-specific antibody detection for seroepidemiology: a multiplex analysis approach accounting for accurate seroprevalence. *J Infect Dis* **222**, 1452–1461.
- Horndler, L., Delgado, P., Abia, D., Balabanov, I., Martínez-Fleta, P., Cornish, G., Llamas, M.A., Serrano-Villar, S. et al. (2021) Flow cytometry multiplexed method for the detection of neutralizing human antibodies to the native SARS-CoV-2 spike protein. *EMBO Mol Med* **13**, 1–15.
- Hu, B., Guo, H., Zhou, P. and Shi, Z.-L. (2020) Characteristics of SARS-CoV-2 and COVID-19. *Nat Rev Microbiol* **19**, 141–154.
- Huergo, L.F., Selim, K.A., Conzentino, M.S., Gerhardt, E.C.M., Santos, A.R.S., Wagner, B., Alford, J.T., Deobald, N. et al. (2021) Magnetic bead-based immunoassay allows rapid, inexpensive, and quantitative detection of human SARS-CoV-2 antibodies. *ACS Sens* **6**, 703–708.
- Klöpffel, J., Koros, R.C., Dehne, K., Ungerer, M., Würstle, S., Mautner, J., Feuerherd, M., Protzer, U. et al. (2021) Automated, flow-based chemiluminescence microarray immunoassay for the rapid multiplex detection of IgG antibodies to SARS-CoV-2 in human serum and plasma (CoVrapid CL-MIA). *Anal Bioanal Chem* **413**, 5619–5632.
- Lapuente, D., Maier, C., Irrgang, P., Hübner, J., Peter, A.S., Hoffmann, M., Ensser, A., Ziegler, K. et al. (2020) Rapid response flow cytometric assay for the detection of antibody responses to SARS-CoV-2. *Eur J Clin Microbiol Infect Dis* **40**, 751–759.
- Leung, D., Tam, F., Ma, C., Chan, P., Cheung, J., Niu, H., Tam, J. and Lim, P. (2004) Antibody response of patients with severe acute respiratory syndrome (SARS) targets the viral nucleocapsid. *J Infect Dis* **190**, 379–386.
- Long, Q.-X., Liu, B.-Z., Deng, H.-J., Wu, G.-C., Deng, K., Chen, Y.-K., Liao, P.U., Qiu, J.-F. et al. (2020) Antibody responses to SARS-CoV-2 in patients with COVID-19. *Nat Med* **26**, 845–848.
- Mariën, J., Ceulemans, A., Michiels, J., Heyndrickx, L., Kerkhof, K., Foque, N., Widdowson, M.-A., Mortgat, L. et al. (2021) Evaluating SARS-CoV-2 spike and nucleocapsid proteins as targets for antibody detection in severe and mild COVID-19 cases using a Luminex bead-based assay. *J Virol Methods* **288**, 1–6.
- Meyer, B., Drosten, C. and Müller, M.A. (2014) Serological assays for emerging coronaviruses: Challenges and pitfalls. *Virus Res* **194**, 175–183.

- Morgan, E., Varro, R., Sepulveda, H., Ember, J.A., Apgar, J., Wilson, J., Lowe, L., Chen, R. *et al.* (2004) Cytometric bead array: a multiplexed assay platform with applications in various areas of biology. *Clin Immunol* **110**, 252–266.
- Munitz, A., Edry-Botzer, L., Itan, M., Tur-Kaspa, R., Dicker, D., Marcovicu, D., Goren, M.G., Mor, M. *et al.* (2021) Rapid seroconversion and persistent functional IgG antibodies in severe COVID-19 patients correlates with an IL-12p70 and IL-33 signature. *Sci Rep* **11**, 1–13.
- Norman, M., Gilboa, T., Ogata, A.F., Maley, A.M., Cohen, L., Busch, E.L., Lazarovits, R., Mao, C.-P. *et al.* (2020) Ultrasensitive high-resolution profiling of early seroconversion in patients with COVID-19. *Nat Biomed Eng* **4**, 1180–1187.
- Okba, N.M.A., Müller, M.A., Li, W., Wang, C., GeurtsvanKessel, C.H., Corman, V.M., Lamers, M.M., Sikkema, R.S. *et al.* (2020) Severe acute respiratory syndrome coronavirus 2-specific antibody responses in coronavirus disease patients. *Emerg Infect Dis* **26**, 1478–1488.
- Padoan, A., Sciacovelli, L., Basso, D., Negrini, D., Zuin, S., Cosma, C., Faggian, D., Matricardi, P. *et al.* (2020) IgA-Ab response to spike glycoprotein of SARS-CoV-2 in patients with COVID-19: a longitudinal study. *Clin Chim Acta* **507**, 164–166.
- Petherick, A. (2020) Developing antibody tests for SARS-CoV-2. *Lancet* **395**, 1101–1102.
- Russell, M.W., Moldoveanu, Z., Ogra, P.L. and Mestecky, J. (2020) Mucosal immunity in COVID-19: a neglected but critical aspect of SARS-CoV-2 infection. *Front Immunol* **11**, 1–5.
- Sen-Crowe, B., McKenney, M. and Elkbuli, A. (2021) COVID-19 laboratory testing issues and capacities as we transition to surveillance testing and contact tracing. *Am J Emerg Med* **40**, 217–219.
- Simard, C., Richard, J., Bazin, R., Finzi, A. and Trepanier, P. (2022) Standardization of a flow cytometry SARS-CoV-2 serologic test. *Cytotechnology* **74**, 99–103.
- Sterlin, D., Mathian, A., Miyara, M., Mohr, A., Anna, F., Claër, L., Quentric, P., Fadlallah, J. *et al.* (2021) IgA dominates the early neutralizing antibody response to SARS-CoV-2. *Sci Transl Med* **13**, 1–10.
- To, K.-W., Tsang, O.-Y., Leung, W.-S., Tam, A.R., Wu, T.-C., Lung, D.C., Yip, C.-Y., Cai, J.-P. *et al.* (2020) Temporal profiles of viral load in posterior oropharyngeal saliva samples and serum antibody responses during infection by SARS-CoV-2: an observational cohort study. *Lancet* **20**, 565–574.
- Vashist, S.K. (2020) In vitro diagnostic assays for COVID-19: recent advances and emerging trends. *Diagnostics* **10**, 1–7.
- Welch, N.G., Scoble, J.A., Muir, B.W. and Pigram, P.J. (2017) Orientation and characterization of immobilized antibodies for improved immunoassays (Review). *Biointerphases* **12**, 1–14.
- Yu, H.-Q., Sun, B.-Q., Fang, Z.-F., Zhao, J.-C., Liu, X.-Y., Li, Y.-M., Sun, X.-Z., Liang, H.-F. *et al.* (2020) Distinct features of SARS-CoV-2-specific IgA response in COVID-19 patients. *Eur Respir J* **56**, 1–4.
- Zeng, W., Ma, H., Ding, C., Yang, Y., Sun, Y., Huang, X., He, W., Xiang, Y. *et al.* (2021) Characterization of SARS-CoV-2-specific antibodies in COVID-19 patients reveals highly potent neutralizing IgA. *Signal Transduct Target Ther* **6**, 1–3.
- Zhu, H., Hu, S., Jona, G., Zhu, X., Kreiswirth, N., Willey, B.M., Mazzulli, T., Liu, G. *et al.* (2006) Severe acute respiratory syndrome diagnostics using a coronavirus protein microarray. *Proc Natl Acad Sci* **103**, 4011–4016.

## Supporting Information

Additional Supporting Information may be found in the online version of this article:

**Figure S1.** (a) Antibodies profile of each sample.  
**Table S1.** ROC curve analysis using MedCalc.